



Missouri University of Science and Technology
Scholars' Mine

Physics Faculty Research & Creative Works

Physics

01 Jan 2005

The Effect of Cu-Doping on the Magnetic and Transport Properties of $\text{La}_{0.7}\text{Sr}_{0.3}\text{MnO}_3$

M. S. Kim

Jinbo Yang


Qingsheng Cai

X.-D. Zhou

Missouri University of Science and Technology

et. al. For a complete list of authors, see https://scholarsmine.mst.edu/phys_facwork/400

Follow this and additional works at: https://scholarsmine.mst.edu/phys_facwork

 Part of the [Chemistry Commons](#), [Materials Science and Engineering Commons](#), and the [Physics Commons](#)

Recommended Citation

M. S. Kim et al., "The Effect of Cu-Doping on the Magnetic and Transport Properties of $\text{La}_{0.7}\text{Sr}_{0.3}\text{MnO}_3$," *Journal of Applied Physics*, American Institute of Physics (AIP), Jan 2005.
The definitive version is available at <https://doi.org/10.1063/1.1860992>

This Article - Journal is brought to you for free and open access by Scholars' Mine. It has been accepted for inclusion in Physics Faculty Research & Creative Works by an authorized administrator of Scholars' Mine. This work is protected by U. S. Copyright Law. Unauthorized use including reproduction for redistribution requires the permission of the copyright holder. For more information, please contact scholarsmine@mst.edu.

The effect of Cu-doping on the magnetic and transport properties of $\text{La}_{0.7}\text{Sr}_{0.3}\text{MnO}_3$

M. S. Kim, J. B. Yang, and P. E. Parris

Department of Physics, University of Missouri-Rolla, Rolla, Missouri 65409 and Graduate Center for Materials Research, University of Missouri-Rolla, Rolla, Missouri 65409

Q. Cai

Department of Physics, University of Missouri-Columbia, Columbia, Missouri 65211

X. D. Zhou, W. J. James, and W. B. Yelon

Graduate Center for Materials Research, University of Missouri-Rolla, Rolla, Missouri 65409

D. Buddhikot and S. K. Malik

Tata Institute of Fundamental Research, Colaba, Mumbai 400-005, India

(Presented on 8 November 2004; published online 11 May 2005)

The effects of Cu-doping on the structural, magnetic, and transport properties of $\text{La}_{0.7}\text{Sr}_{0.3}\text{Mn}_{1-x}\text{Cu}_x\text{O}_3$ ($0 \leq x \leq 0.20$) have been studied using neutron diffraction, magnetization, and magnetoresistance (MR) measurements. All samples show the rhombohedral structure with the $R\bar{3}c$ space-group from 10 K to room temperature (RT). Neutron diffraction data suggest that some of the Cu ions have a Cu^{3+} state in these compounds. The substitution of Mn by Cu affects the Mn–O bond length and Mn–O–Mn bond angle resulting from the minimization of the distortion of the MnO_6 octahedron. Resistivity measurements show that a metal to insulator transition occurs for the $x \geq 0.15$ samples. The $x=0.15$ sample shows the highest MR ($\approx 80\%$), which might result from the co-existence of Cu^{3+} – Cu^{2+} and the dilution effect of Cu-doping on the double exchange interaction. © 2005 American Institute of Physics. [DOI: 10.1063/1.1860992]

I. INTRODUCTION

The ABO_3 (A=trivalent rare earth atom, B=divalent alkaline metal) perovskites have attracted considerable attention because of the anomalous magnetic and transport properties such as colossal magnetoresistance (CMR), and metal–insulator transitions (MIT).^{1–3} The $\text{La}_{1-x}\text{Sr}_x\text{MnO}_3$ perovskites are a canonical ABO_3 -type, CMR material. It has been reported that double-exchange (DE) interactions together with Jahn–Teller (JT) distortions in the MnO_6 octahedron may be required to account for the large MR effects.^{4–7} Because the Mn ion is the center of the DE interaction, the role of the Mn atom and its local environment have become the focus of much of the research on manganese perovskites. To investigate the CMR associated with the lattice deformation and charge ordering of the crucial Mn–O–Mn network, many early studies were carried out by doping the A-site with divalent atoms (Ca, Sr, Ba, etc).^{8–10} Recently, it has also been shown that substitution of Mn(B-site) by other atoms dramatically affects the magnetic and transport properties of manganese perovskites.^{11–14} The B site modification directly affects the Mn network by changing the Mn^{3+} – Mn^{4+} ratio and the electron carrier density, which may provide a better understanding of the mechanism for CMR effects in the perovskites.

In this study, we report the effects of replacing Mn with Cu on the structural, magnetic and transport properties of $\text{La}_{0.7}\text{Sr}_{0.3}\text{Mn}_{1-x}\text{Cu}_x\text{O}_3$ with $0 \leq x \leq 0.20$.

II. EXPERIMENTAL

Samples of Cu-substituted $\text{La}_{0.7}\text{Sr}_{0.3}\text{Mn}_{1-x}\text{Cu}_x\text{O}_3$, with $0 \leq x \leq 0.20$, were prepared using the conventional solid state reaction method. X-ray diffraction of the powders was carried out at RT using a SCINTAG diffractometer with Cu–K α radiation. Powder neutron diffraction experiments were performed at the University of Missouri-Columbia Research Reactor(MURR) using neutrons of wavelength $\lambda=1.4875$ Å. Refinement of the neutron diffraction data was carried out using the FULLPROF program.¹⁶ Magnetic measurements

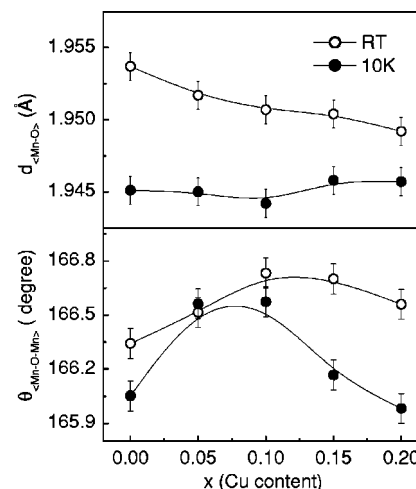


FIG. 1. Average (Mn, Cu)–O bond lengths $d_{\text{Mn-O}}$ (a), (Mn, Cu)–O–(Mn, Cu) bond angles $\theta_{\text{Mn-O-Mn}}$ (b) of $\text{La}_{0.7}\text{Sr}_{0.3}\text{Mn}_{1-x}\text{Cu}_x\text{O}_3$ ($x=0, 0.05, 0.10, 0.15, 0.20$) at room temperature and at 10 K.

TABLE I. Refined parameters for $\text{La}_{0.7}\text{Sr}_{0.3}\text{Mn}_{1-x}\text{Cu}_x\text{O}_3$, $R\bar{3}c$ space-group, at room temperature and $T=10$ K. Numbers in parentheses are statistical errors. a and c are the lattice parameters. m is magnetic moment. V is the unit cell volume. χ^2 is $[R_{\text{wp}}/R_{\text{exp}}]^2$ where R_{wp} is the residual error of the weighted profile. The magnetic moments of the $x \geq 0.15$ samples at RT are not refined.

Composition (x)	0.00	0.05	0.10	0.15	0.20
$T=300$ K					
a (Å)	5.5038(2)	5.5003(2)	5.4987(2)	5.4982(2)	5.4941(2)
c (Å)	13.3552(5)	13.3387(4)	13.3341(5)	13.3304(6)	13.3180(6)
V (Å ³)	350.351(18)	349.473(17)	349.153(18)	348.990(22)	348.152(24)
m (μ_B)	2.512(28)	1.975(30)	1.411(101)
χ^2 (%)	2.81	2.69	2.91	4.89	5.36
$T=10$ K					
a (Å)	5.4812(1)	5.4845(1)	5.4823(1)	5.4858(1)	5.4855(2)
c (Å)	13.2759(3)	13.2797(4)	13.2737(4)	13.2718(4)	13.2637(4)
V (Å ³)	345.415(13)	345.931(16)	345.504(17)	345.897(17)	345.642(17)
m (μ_B)	3.445(24)	3.327(27)	3.160	2.272(50)	0.727(93)
χ^2 (%)	3.18	2.76	3.30	2.67	2.82

were conducted with a SQUID magnetometer and resistivity data were obtained using a physical properties measurement system (PPMS) with a standard four-point probe method.

III. RESULTS AND DISCUSSION

X-ray diffraction studies of $\text{La}_{0.7}\text{Sr}_{0.3}\text{Mn}_{1-x}\text{Cu}_x\text{O}_3$ samples with $0 \leq x \leq 0.20$ indicate that all samples are single phase and all peak positions can be indexed to $\text{La}_{0.67}\text{Sr}_{0.33}\text{MnO}_{2.91}$ (JCPDS 50-0308). To further investigate the structure distortion and magnetic properties of these compounds, powder neutron diffraction data were collected at RT and 10 K. All patterns can be fitted well with the $R\bar{3}c$ rhombohedral space-group (No.167). Refined lattice parameters and magnetic moments for the compounds are listed in Table I. At RT, the lattice parameters a, c , and the unit cell volumes decrease with increasing Cu content. At 10 K, the lattice parameters and unit cell volume remain nearly constant with increasing Cu content. The refined magnetic moments of Mn atoms at 10 K and RT decrease with increasing Cu content. These results agree well with the values obtained from magnetic measurements.

Generally, the B-site doping will directly change the $\text{Mn}^{3+}-\text{Mn}^{4+}$ ratio and the exchange interaction of Mn–Mn. The lattice parameters and crystal structure will be affected due to the mismatch of the ionic radius between the Mn ions and the doping ions. Even though the most stable state of Cu is Cu^{2+} , the Cu^{2+} (6 coordination) radius is about 0.73 Å, which is much larger than the radius of Mn^{3+} (0.645 Å) and Mn^{4+} (0.53 Å).¹⁵ The substitution of Mn by Cu^{2+} will lead to an expansion of the unit cell rather than a contraction. Therefore, the decrease of the unit cell volume with Cu-doping at RT suggests that some of the Cu ions are in a Cu^{3+} state with a radius of 0.54 Å, which is smaller than that of Mn^{3+} and larger than that of Mn^{4+} .

That might be the reason that the changes of the unit cell volume and the lattice parameters are not linear with Cu content. A similar phenomenon has been observed in $(\text{La}, \text{Ba})\text{Cu}_{1-x}\text{Mn}_x\text{O}_3$ compounds, where Cu^{3+} enters Mn sites.¹⁴

The average (Mn, Cu)–O bond length and (Mn, Cu)–O–(Mn, Cu) bond angle extracted from the Rietveld refinements

are shown in Fig. 1. At RT, the average bond length decreases gradually while the average bond angle increases up to $x=0.10$ then slightly decreases for $x \geq 0.15$. At 10 K, the average bond length decreases up to $x=0.1$ and remains constant for $x \geq 0.15$, while the average bond angle increases and attains a maximum value at $x=0.10$. The average bond length and the average bond angle are directly related through the oxygen positions and content. The refinement results indicate that there is no oxygen deficiency within error limits. Therefore, the unusual changes in the average (Mn, Cu)–O bond length and (Mn, Cu)–O–(Mn, Cu) bond angle between RT and 10 K might be related to the magnetostriction that reflects the magnetic ordering temperature and the existence of mixed $\text{Cu}^{2+}-\text{Cu}^{3+}$ states. The internal strain in the MnO_6 octahedron may be released by a small distortion of the MnO_6 octahedra through changes in bond length and bond angle.

Figure 2 shows the magnetization versus temperature (M-T) curves measured under field cooling (FC) and zero field cooling (ZFC) conditions in a magnetic field of 50 Oe for the $x=0.05, 0.10$, and 0.15 samples. Two magnetic transition temperatures are shown for the samples with $x=0.05$

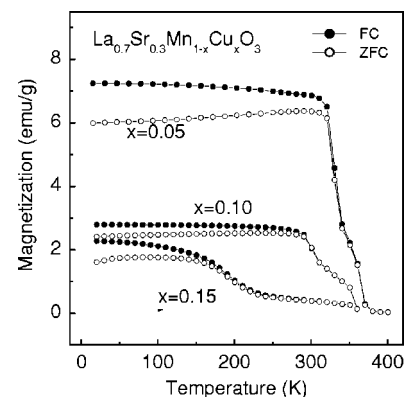


FIG. 2. The magnetization vs temperature (M-T) curves of $\text{La}_{0.7}\text{Sr}_{0.3}\text{Mn}_{1-x}\text{Cu}_x\text{O}_3$ ($x=0.05, 0.10, 0.15$) measured under field cooling (FC) and zero field cooling (ZFC) conditions in a magnetic field of 50 Oe.

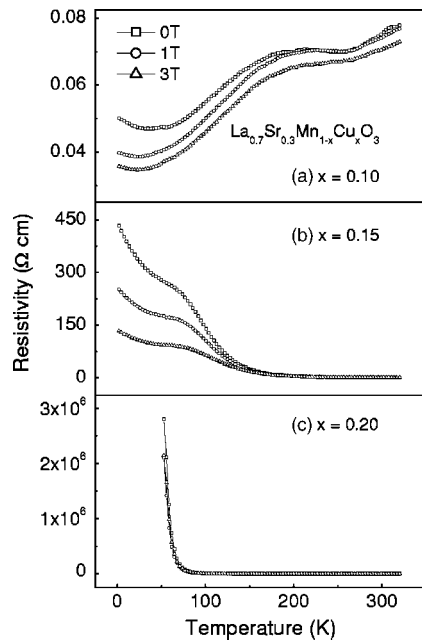


FIG. 3. Electric resistivity ρ vs temperature for $\text{La}_{0.7}\text{Sr}_{0.3}\text{Mn}_{1-x}\text{Cu}_x\text{O}_3$ [$x=0.10$ (a), 0.15 (b), 0.20 (c)] in applied magnetic field $H=0,1,3,5$ T.

and 0.10. The neutron diffraction data do not show the presence of other phases in the Cu-doped samples within the resolution of neutron diffraction analysis.

Figure 3 shows the temperature dependence of resistivity under various fields for $\text{La}_{0.7}\text{Sr}_{0.3}\text{Mn}_{1-x}\text{Cu}_x\text{O}_3$ ($x=0.10, 0.15$, and 0.20). With increasing Cu content, the resistivity of the compound increases, while the resistivity decreases with increasing magnetic field. This is ascribed to a reduction of the $\text{Mn}^{3+}-\text{Mn}^{4+}$ ratio to account for the DE interaction and a reduction in the number of hopping electrons and hopping sites by Cu substitution. In addition, Cu^{3+} has 8 electrons in the d -orbital, and is highly localized with a strong Coulomb repulsion. Therefore, the $\text{Mn}^{3+} e_{g\uparrow}^1$ electron may not itinerate through the $\text{Mn}^{3+}-\text{Cu}^{3+}$ chains but through the antiferromagnetic super-exchange chains of $\text{Mn}^{3+}-\text{Mn}^{3+}$ and $\text{Mn}^{4+}-\text{Mn}^{4+}$. Therefore, Cu substitution weakens the DE interaction, disturbs the Mn–O–Mn network, and creates short range ordered ferromagnetic clusters. As more Cu is substituted, more inhomogeneous small clusters are formed, leading to a broadening of the magnetic phase transition peak.

For the $x \leq 0.10$ samples, metallic behavior is shown with decreasing temperature and for the samples with $x \geq 0.15$, a metal–insulator transition (MIT) appears (see Fig. 2). A resistivity peak corresponding to the magnetic transition is present. There is no clear field-induced shift of maximum resistivity for all samples. The suppression of the resistivity by the applied magnetic field occurs over the entire temperature range for all samples. In the DE mechanism, the

mobility of the charge carrier e_g electrons improves if the localized spins are polarized. The applied field aligns the canted electron spins which should reduce the scattering of itinerant electrons with spins and thus the resistivity is reduced. The temperature dependence of the magnetoresistance was calculated with $[\text{MR}=(\rho_0-\rho_H)/\rho_0 \times 100]$ under $H=1, 3$, and 5 T. The MR increases with increasing Cu content up to $x \leq 0.15$ samples and shows the maximum MR = 80% below $T=100$ K, for the $x=0.15$ sample. The maximum MR decreases with further Cu-doping.

In summary, we have investigated the structural, magnetic and electronic properties of Cu-doped $\text{La}_{0.7}\text{Sr}_{0.3}\text{Mn}_{1-x}\text{Cu}_x\text{O}_3$. All samples show the same crystal structure from 10 K to RT. The variations of the bond length and bond angle resulting from Cu substitution minimize the distortion of the MnO_6 network and stabilize the rhombohedral structure. A mixture of Cu^{2+} and Cu^{3+} ions gives rise to a decrease of the unit cell volume and a change of the Mn valence states in these compounds. The metal to insulator transition for the samples with $x \geq 0.15$ results from changes in the Mn–O–Mn interaction, Mn valence state and the charge carrier concentration in the Cu-doped compounds.

ACKNOWLEDGMENTS

We thank Aranwela Hemantha for invaluable help with the magnetoresistance measurements. The support by DOE under DOE Contract No. DE-FC26-99FT400054 is acknowledged.

- ¹J. B. Goodenough, *Magnetism and the Chemical Bond* (Interscience, New-York/London 1963).
- ²A. Unishibara, Y. Moritomo, T. Arima, A. Asamitsu, G. Kido, and Y. Tokura, *Phys. Rev. B* **51**, 14103 (1995).
- ³Y. Tomioka, A. Asamitsu, H. Kuwahara, and Y. Tokura, *Phys. Rev. B* **53**, R1689 (1996).
- ⁴C. Zener, *Phys. Rev.* **82**, 403 (1951).
- ⁵P. W. Anderson and H. Hasegawa, *Phys. Rev.* **100**, 675 (1955).
- ⁶K. Kubo and N. Ohata, *J. Phys. Soc. Jpn.* **33**, 21 (1972).
- ⁷A. J. Millis, P. B. Littlewood, and B. I. Shraiman, *Phys. Rev. Lett.* **74**, 5144 (1995).
- ⁸J. J. Neumeier, K. Andres, and K. J. McClenllan, *Phys. Rev. B* **59**, 1701 (1999).
- ⁹M. Medarde, J. Mesot, P. Lacorre, S. Rosenkranz, P. Fischer, and K. Go-brecht, *Phys. Rev. B* **52**, 9248 (1995).
- ¹⁰D. Cao, F. Bridges, M. Anderson, A. P. Ramirez, M. Olapinski, M. A. Subramanian, C. H. Booath, and G. H. Kwei, *Phys. Rev. B* **64**, 184409 (2001).
- ¹¹C. Martin, A. Maignan, and B. Raveau, *J. Mater. Chem.* **6**, 1245 (1996).
- ¹²J. Blasco, J. Garcia, J. M. De Teresa, M. R. Ibarra, J. Perez, P. A. Algarabel, and C. Marquina, *Phys. Rev. B* **55**, 8905 (1997).
- ¹³K. H. Ahn, X. W. Wu, K. Liu, and C. L. Chien, *J. Appl. Phys.* **81**, 5505 (1997).
- ¹⁴S. L. Yuan, Y. Jiang, G. Li, J. Q. Li, Y. P. Yang, M. X. Y. Zhang, P. Tang, and Z. Huang, *Phys. Rev. B* **61**, 3211 (2004).
- ¹⁵R. D. Shannon, *Acta Crystallogr., Sect. A: Cryst. Phys., Diff., Theor. Gen. Crystallogr.* **32**, 751 (1976).
- ¹⁶J. Rodriguez-Carvajal, Program: FULLPROF, Version 3.5d.